arXiv:1609.04661v1 [cs.DS] 15 Sep 2016

Denoising Message Passing for X-ray Computed Tomography Reconstruction

Alessandro Perelli, Michael Lexa, Ali Can and Mike Davies, *Fellow, IEEE*

***Abstract*—X-ray Computed Tomography (CT) reconstruction from sparse number of views is becoming a powerful way to reduce either the radiation dose or the acquisition time in CT systems but still requires a huge computational time. This paper introduces an approximate Bayesian inference framework for CT reconstruction based on a family of denoising approximate message passing (DCT-AMP) algorithms able to improve both the convergence speed and the reconstruction quality. Approximate Message Passing for Compressed Sensing has been extensively analysed for random linear measurements but there are still not clear solutions on how AMP should be modified and how it performs with real world problems. In particular to overcome the convergence issues of DCT-AMP with structured measurement matrices, we propose a disjoint preconditioned version of the algorithm tailored for both the geometric system model and the noise model. In addition the Bayesian DCT-AMP formulation allows to measure how the current estimate is close to the prediction by analysing the state evolution. This work aims to provide a proof of concept to demonstrate that approximate Bayesian reconstruction algorithms can be tailored for ill conditioned, underdetermined real problems such CT imaging. Experiments with simulated and real CT baggage scans confirm that the performance of the proposed algorithms are comparable and can even outperform traditional statistical X-ray CT reconstruction optimization solvers.**

***Keywords*—X-ray Computed Tomography, Compressed Sensing, Approximate Message Passing, Image denoising, Preconditioning, Iterative algorithms**

I. Introduction

X-ray Computed Tomography (CT) is one of the widely used imaging techniques for medical diagnosis, image-guided radiotherapy, material characterization and security applications. However reducing X-ray radiation exposure is a paramount concern in particular for diagnostic CT where patients are subjected to repeated scans. Furthermore, especially for material analysis and explosives detection, new generation CT scanners are employing Dual Energy (DE) systems to enhance material discrimination. This tends to either reduce the acquisition data per energy or increase the acquisition time. To lower the X-ray dose, two different strategies can be implemented: reducing the X-ray flux toward each detector element, i.e. the milliampere per seconds (low-mAs) per projection, or decrease the number of projections (sparse-views) per rotation. While for speeding up scans fixed gantry systems have been proposed [1] which inevitably reduce the range of projections that can be acquired. In this work we are primarily focusing on sparse views CT since it can be fruitfully utilised either to reduce the dose in medical CT and reduce the acquisition time in DE scans. CT Image reconstruction, from sparse views acquisitions, achieved by conventional filtered back projection (FBP) algorithms is generally affected by a high degree of noise and noticeable streeking artifacts that are not acceptable for diagnostic purposes. Many approaches have been proposed to solve the linear CT problem. In particular state of the art statistical CT image reconstruction, aims to minimize a cost function defined as a sum of a data fidelity term that takes into account the measurements statistical model, the geometry of the CT acquisition and a regularization term that imposes a prior model on the solution. Generally the cost function for X-ray CT is defined considering the negative log-likelihood function [2] or a penalized weighted least-squares (PWLS) cost function with a weighted quadratic approximation of the Poisson noise model [3]. Several types of iterative algorithms have been designed to solve the statistical X-ray CT problem but in general current methods require many iterations to converge yielding a high computation time not suitable for clinical/industrial CT uses. However iterative methods can provide images with enhanced resolution and reduced artifacts compared to low dose FBP [4]. A large number of iterative algorithms have been utilised for statistical CT reconstruction, among these coordinate descent [5], preconditioned conjugate gradient [6] and ordered subset [7]. Recently researchers have developed new algorithms with faster convergence by using splitting techniques [8], alternating direction method of multipliers based algorithm [9] or combining Nesterov momentum techniques with ordered subsets to accelerate gradient descent methods [10]. Nesterov momentum techniques can achieve a convergence rate $\mathcal{O}(\frac{1}{t^2})$ where t is the number of iterations, however due to the large Lipschitz constant of the gradient term this method does not show significant improvement compared to previous algorithms [8]. In general any first-order iterative methods require at each iteration the computation of the forward and back projection operator which represent the main contribution to computation time. In order to accelerate the reconstruction it is necessary to either design faster CT operators or develop iterative algorithms that can converge in fewer iterations. This paper will focus primarily on the latter.

In this work we propose a new CT image reconstruction algorithm based on the Bayesian framework using Approximate Message passing (AMP). AMP based inference refers to a family of iterative algorithms first proposed in [11] for Compressed Sensing problems or solving underdetermined linear systems with an i.i.d. random Gaussian system matrix

A. Perelli and M. Davies are with the Institute for Digital Communications (IDCOM), The University of Edinburgh. EH9 3JL, United Kingdom e-mail: a.perelli@ed.ac.uk, mike.davies@ed.ac.uk

M. Lexa and A. Can are with the GE Research Center, Niskayuna, United States e-mail: lexa@ge.com, can@ge.com

and a sparse signal model. In particular with the Generalized Linear Model (GLM) and an i.i.d. Gaussian system matrix with entries of zero mean and variance $\frac{1}{N}$ where N in the image space dimension, it has been shown that AMP has superior performance to existing CS algorithms and it is proven to converge in few iterations. Furthermore AMP tends to the Minimum Mean Square Error (MMSE) estimator in the large system limit, i.e. the estimate follows the predicted MMSE through the analysis of the state evolution [11]. The original derivation of AMP is based on the Belief Propagation (BP) framework and used the central limit theorem and Taylor expansion to simplify the message computation.

A key criticism leveled at AMP and its generalizations is that it is a specialist algorithm for i.i.d. based measurement matrices and hence it is unclear to what extent it can be applied to real word sensing problems. There has been some work exploring the convergence properties of AMP and its generalizations to other matrix classes [12] and linking the algorithm with more classical optimization strategies such as ADMM [13]. Similarly there exist strategies for stabilizing the algorithm like damping technique that has been investigated and employed on AMP for hyperspectral imaging reconstructions with empirical convergence results [14]. Alternatively, in [15] a novel S-AMP algorithm, an extension of AMP to general random matrices, has been proposed but the algorithm requires the calculation of the S-transform of the Gram matrix which is computationally expensive and non-trivial.

The aim of the current paper is to answer the question whether such algorithms can provide good approximate Bayesian inference for real world problems, in particular CT image reconstruction.

A. Main Contribution

Our approach to developing an AMP based algorithm for CT reconstruction builds on a number of recent developments in AMP algorithms and in particular makes use of the following key points:

- design of a good preconditioner for the system based on the forward measurement model;
- incorporation of the Poisson noise model through the Generalized AMP formulation (GAMP)
- incorporation in AMP of a broader class of signal prior rather than sparse signal models through the D-AMP framework to enable the use of generic nonlinear functions/denoisers which can be applied to the image estimate at each iteration;
- demonstration that the predicted MSE still provides a reasonable estimate, even in this non-random setting.

As far as the authors are aware, this is the first work aimed to design a Denoising Message Passing based algorithm for CT reconstruction.

A key challenge of applying AMP for CT reconstruction is due to the fact that the measurement matrix, A, for example the Radon matrix for parallel beam geometry, is very ill-conditioned which would require a significant level of damping and the subsequent reduction is convergence rate. [12]. The main idea is to map the non tight Radon operator in the image domain to a new better conditioned operator by preconditioning, exploiting, as has been done in previous iterative CT reconstruction, the filtered back projection property of the system model [16]. The same procedure can be applied for different CT geometries like 2D fan-beam and 3D helical. The above mentioned preconditioning procedure applies only to the system operator and therefore requires the modeling of the Poisson statistics to be dealt with separately. This we can do using the Generalized AMP (GAMP) framework [17], which represents an extension of AMP, that allows the incorporation of arbitrary noise models. Finally the further extension of GAMP, subsequently called DCT-AMP, employs a broader, generic prior distribution on $\mathbf{x}$ rather than simply a sparse factorizable prior distribution [18]. A key element of GAMP is that it retains the so-called Onsager term which helps avoid the build up of correlations in the error across iterations and therefore enables the algorithm to accurately estimate the MSE within the algorithm iterations. We will see that the flexibility of using generic denoisers at each iteration of the GAMP yields to a better reconstruction of the image structure compared to more simple regularization.

B. Structure of the paper

The remainder of this paper is structured as follows: Section II describes the X-ray CT absorption-based mathematical model and introduces the approximations that lead to the classical PWLS statistical CT reconstruction problem. It then explains how the DCT-AMP framework can be related to this statistical formulation. Section III analyses the DCT-AMP algorithm and explains the system preconditioning for CT and the issues of incorporating the noise model as a preconditioner in the sinogram (measurement) domain. Section V establishes a connection between our state evolution and existing state evolutions. Finally, in Section VI comprehensive results on DCT-AMP CT reconstruction on experimental acquisitions of cargo luggage are shown together with a comparison of its performance with state-of-the-art algorithms in model-based CT reconstruction.

II. X-ray Computed Tomography Model

X-ray CT produces images of the X-ray attenuation coefficients of the object or patient being scanned. A typical construction of an X-ray scanner involves a source and a detector array. The source is an incoherent source of X-ray radiation and detectors record the intensity of the radiation exiting the patient. Let N be the total number of such source positions and detector element pairs and i be the index numbering them. If the intensity of this beam of radiation, before, I_0, and after, I_i, passing through the patient is known, then Beer's law provides the total attenuation experienced by the beam:

$$I_i = I_0 e^{-\int_{L_i} \mu(r) dr} \tag{1}$$

where, L_i is the path of the ray through the patient and $\mu(r)$ is the distribution of X-ray attenuation coefficients in the patient as a function of position in the co-ordinate system. Eq. (1) assumes that the X-ray photons in an X-ray beam have the same energy, i.e., the X-rays used are monoenergetic.

The noise model is composed of (a) a compound Poisson and (b) a compound Poisson with Gaussian readout noise. However, the simple Poisson model has generally been found to be satisfactory in current practice. For a source-detector-pair, i, let I_0 denote the initial intensity of the beam expressed as number of counts and let ϵ_i the expected value for the electronic read-out noise and scatter (while the observations may also be effected by other physical processes such as beam hardening, these are generally accounted for using appropriate sinogram precorrection techniques that we will expand upon below). The observations are thus random variables assumed to be Poisson-distributed with mean as:

$$y_i = \text{Poisson}\{I_0 e^{-\int_{L_i} \mu(r) dr} + \epsilon_i\} \tag{2}$$

The Beer's law as modeled in Eq. (2) does not hold with polychomatic sources and does not model beamhardening. Beam hardening is the phenomenon in which the mean energy of the photons of an X-ray beam increases as the beam progresses through the body. This happens because the materials that make up the human body attenuate lower energy photons more than higher energy photons. This causes the Beers Law to no longer hold, and has to be replaced as shown below. Neglecting beam hardening in images results in two types of artifacts: cupping and streaks. Some form of beam hardening correction is necessary if an accurate measurement of the X-ray attenuation coefficient is desired [19]. The formulation in Eq. (3) has to be modified for the more practical case of polyenergetic X-rays as follows

$$\begin{aligned} y_i &= \text{Poisson}\left\{\int I_i(E) e^{-\int_{L_i} \mu(r,E) dr} dE + \epsilon_i\right\} \\ &\approx \text{Poisson}\left\{\int I_i(E) e^{-\sum_j \mu_j(E) A_{i,j}} dE + \epsilon_i\right\} \end{aligned} \tag{3}$$

where $I_i(E)$ is the energy spectrum of the incident X-ray and the last expression results from discretizing the linear attenuation function $\mu(x;E)$. $A_{i,j}$ in (3) represents the i,j entry of a matrix A whose numerical value equals the intersection length of ray i with voxel j, and $\mu_j(E)$ is a constant that approximates the value of $\mu(x,E)$ on voxel j. A possibility to simplify Eq. (3) consists in applying a polychromatic-to-monochromatic source correction [20] to (3) to yield

$$\begin{aligned} h(\lambda_i) &= h\left(\int S_i(E) e^{-\sum_j \mu_j(E) A_{i,j}} dE + \epsilon_i\right) \\ &\approx e^{-\sum_j \mu_j(E_0) A_{i,j}} \end{aligned} \tag{4}$$

where $h : \mathbb{R} \to \mathbb{R}$ is a function that adjusts the observation λ_i such that it is as if the source were monochromatic. In practice, h is taken to be a polynomial whose coefficients are found by using calibration scans. Projection values are then modeled as

$$\begin{aligned} y_i &= \text{Poisson}\{\log\left(h(\lambda_i)\right) + \epsilon_i\} \\ &= \text{Poisson}\left\{\sum_j \mu_j(E_0) A_{i,j}\right\} \end{aligned} \tag{5}$$

where in the last equation we have neglected the read-out and scatter noise term ϵ_i. This also leads to the matrix equation $\mathbf{y} = \text{Poisson}\{A\mu\}$.

A. The PWLS formulation of Statistical CT Reconstruction

The PWLS statistical formulation of the CT problem is based on the quadratic approximation to the Poisson likelihood. This is equivalent to assuming an additive Gaussian noise model for the data. This model is reasonable for large SNR in clinical X-ray CT. With high photon flux, PWLS leads to negligible bias and the simpler objective function reduces computation time. The negative log likelihood for CT data is

$$\begin{aligned} -L(\mu) &= \sum_{i=1}^{N} h_i([A\mu]_i) \\ &= \sum_{i=1}^{N} \{-y_i \log(b_i e^{[A\mu]_i} + \epsilon_i) + (b_i e^{[A\mu]_i} + \epsilon_i) \end{aligned} \tag{6}$$

Applying a second-order Taylor's expansion to $h_i(l)$ around some value $\hat{h}_i$ yields [2]:

$$h_i(l) \approx h_i(\hat{l}_i) + \dot{h}_i(\hat{l}_i)(l - \hat{l}_i) + \frac{\ddot{h}_i(\hat{l}_i)}{2}(l - \hat{l}_i)^2 \tag{7}$$

where $\dot{h}_i(\cdot)$ and $\ddot{h}_i(\cdot)$ are respectively the first and second derivatives of h_i. Assuming $y_i > \epsilon_i$, we can estimate the line integral with

$$\hat{l}_i = \log\left(\frac{b_i}{y_i - \epsilon_i}\right)$$

Substituting this estimate into Eq. (7) gives the following approximation for h_i

$$h_i(l) \approx (y_i - y_i \log y_i) + \frac{w_i}{2}(l - \hat{l}_i)^2 \tag{8}$$

The first term is independent of l and can be dropped. The weight is $w_i = \frac{(y_i - \epsilon_i)^2}{y_i}$; with $\epsilon_i \approx 0$ we have $w_i = y_i$. The simplified linear model for PWLS based X-ray Computed Tomography is therefore:

$$\mathbf{y} = \mathbf{A}\mu + \nu \tag{9}$$

where $y = \log(h(\lambda_i)) \in \mathbb{R}^{M \times 1}$ is (post-log) measurement data, $\mathbf{A} \in \mathbb{R}^{M \times N}$ is a forward projection operator, $\mathbf{x} \in \mathbb{R}_+^{N \times 1}$ is an unknown (nonnegative) image of attenuation coefficients to be reconstructed and ν is Gaussian noise $\nu \sim \mathcal{N}(0, 1/\mathbf{y})$ resulting in the following PWLS constrained optimization problem for statistical CT reconstruction:

$$\arg\min_{\mu} \left[\frac{1}{2}\|\mathbf{y} - \mathbf{A}\mu\|_{\mathbf{W}}^2 + \Psi(\mathbf{R}\mu)\right] \quad \text{s.t. } \mu \geq 0 \tag{10}$$

where $\mathbf{y}$ is the $M \times 1$ measurement vector, $\mathbf{A}$ is the $M \times N$ system matrix (or forward operator), $\mathbf{A}\mu$ performs the forward projection, i.e. line integral, μ is the $N \times 1$ vectorized version of the CT image and $\mathbf{W} = \text{diag}\{w_i\}$ is a $M \times M$ diagonal matrix consisting of statistical weights, w_i are inversely proportional to the variance of the measurement i.e. $w_i = e^{-y_i}$. The family of regularizers $\Psi(\mathbf{R}\mu)$ is defined in the analysis form which means that Ψ is described as function of the reconstructed image $\mathbf{x}$.

III. Proposed Method for CT Reconstruction

The main objective of this work is to design fast Denoising Generalized Approximate Message passing (DCT-AMP) based algorithm for X-ray CT reconstruction through a suitable preconditioner which exploit the structure of the measurement operator and incorporating the noise measurement Poisson statistics. Furthermore, DCT-AMP incorporates a broader, generic prior distribution on $\mathbf{x}$ rather than simply a factorizable prior distribution. An instance of estimation problems in a Bayesian setting is considered where an hidden input vector $\mu \in \mathbb{R}$ with a generic prior $p(\mu)$ is passed through the CT forward model that we modelled as a linear transform

$$\mathbf{z} = \mathbf{A}\mu \tag{11}$$

where $\mathbf{A} \in \mathbf{R}^{M\times N}$ is the transform matrix. Finally, each component of z_i randomly generates an output component y_i of a vector $\mathbf{y} \in \mathbb{R}^M$ through a Poisson model with conditional probability density function $p_{Y|Z}(y_i|z_i)$. The reconstruction problem is to estimate the attenuation input μ. In the following we start from describing the AMP iterations considering the model of y where the signal distribution follows $\mu_i \sim p_\mu$ and the noise is i.i.d. Gaussian. We review the standard D-AMP [11] and then we will generalize the framework to incorporate preconditioning for the system operator $\mathbf{A}$, and the Poisson noise model.

D-AMP has been derived considering the linear model where the measurement vector is expressed as $\mathbf{y} = \mathbf{A}\mu + \mathbf{w}$ with $\mathbf{y} \in \mathbb{R}^M$ and $\mathbf{x} \in \mathbb{R}^N$ and noise vector $w \in \mathbb{R}^M$ that we can assume to be i.i.d. Gaussian. The traditional derivation of AMP for the above mentioned linear model has been obtained through the analysis of the associated graphical model.
The noise distribution is given by:

$$p(\mathbf{y}|\mathbf{z}) = \prod_{a=1}^{m} p(y_a|\mathbf{z}) \tag{12}$$

if the noise is assumed to be independent and Gaussian distributed $p(\mathbf{y}|\mathbf{z}) = \mathcal{N}(\mathbf{y}|\mathbf{z}, q^{-1})$ so $p(y_a|\mathbf{z}) \propto e^{-\frac{q}{2}(y_a - z_a)^2}$.

In case the entries of the measurement matrix $\mathbf{A}$ are i.i.d. $\mathcal{N}(0, \frac{1}{M})$ distributed, and thus the columns of the matrix have unit l_2-norm, on average, D-AMP proceeds iteratively according to

$$\begin{aligned} \mu^{t+1} &= D_{\hat{\sigma}^t}(\mathbf{A}^T r^t + \mu^t) \\ \mathbf{r}^t &= \mathbf{y} - \mathbf{A}\mu^t + \frac{1}{R} r^{t-1} D'_{\hat{\sigma}^t}(\mathbf{A}^T \mathbf{r}^{t-1} + \mu^{t-1}) \end{aligned} \tag{13}$$

where $R = M/N$ represents the measurement rate. $D_{\hat{\sigma}^t}(\cdot)$ is a denoising function for the class of signal in $\mathcal{C}$ at the t-th iteration which, as in [18], is required to satisfy the following properties: monotone, proper, Lipschitz continous.

$D'_{\hat{\sigma}^t}$ denotes the expected value of the divergence of the denoiser. The analytic calculation of $D'_{\hat{\sigma}^t}$ is often complicated because many times denoisers do not have an explicit formulation and are in general data-dependent, but a good approximation can be obtained through the Monte Carlo technique [21]. With this method the calculation of the Onsager term is more efficient since it requires only one more application of the denoiser. We highlight that the vector $\mathbf{A}^T\mathbf{r}^t + \mu^t \in \mathbb{R}^N$ in (13) can be regarded as noisy measurements of μ in the t-th iteration with noise variance σ_t^2. A better insight of how the algorithm works can be obtained just rewriting (13):

$$\begin{aligned} \mu^{t+1} &= D_{\hat{\sigma}^t}(\mathbf{s}^t) \\ \mathbf{s}^t &= \mu^t + \mathbf{A}^T \left(\mathbf{y} - \mathbf{A}\mu^t + \frac{1}{R} \frac{\mathbf{s}^{t-1} - \mu^{t-1}}{\mathbf{A}^T} D'_{\hat{\sigma}^t}(\mathbf{s}^{t-1}) \right) \end{aligned} \tag{14}$$

which highlights how the D-AMP algorithm is composed of:

- a "modified" gradient descent step where the estimate μ^t is updated along the gradient plus an additional term, the so called "Onsager term", which is linked with the previous estimate, and
- a denoising step of the current estimate μ^t

The main reason for using generic denoiser in the non linear step is to capture the data-dependent structure of complex images rather than a simple factorial model, obtaining a sequence of estimates eventually converging faster to the true image μ_0.
The motivation for D-AMP is to try to exploit the huge number of image denoisers available to enhance the AMP algorithm. The main challenge for AMP-based algorithms is the lack of convergence proofs in case of structured system matrices $\mathbf{A}$ like in the case of X-ray CT.

A possible solution to enforce the convergence of the message passing algorithm, for example used for hyperspectral imaging [14], is to introduce a damping factor on both the image estimate x^t and the residual r^t such that we have a weighted average, with $\alpha \in [0, 1]$

$$\begin{aligned} \mathbf{r}^t &= (1-\alpha)\mathbf{r}^t + \alpha \mathbf{r}^{t-1} \\ \mu^t &= (1-\alpha)\mu^t + \alpha \mu^{t-1} \end{aligned} \tag{15}$$

In this work we propose an alternative way of enforcing convergence based on exploiting a preconditioning scheme which exploits the structure of the forward and backward CT operator and measurement noise statistics.

A. Preconditioning using Cone Filter

Designing proper preconditioners for AMP is generally challenging and even more difficult for X-ray CT because of the large dynamic range of the measurements which causes the Hessian of the statistical data-fidelity term to be highly shift-variant [6]. Our choice for the preconditioner of the proposed AMP algorithm is strictly connected with the geometry of the CT system. In particular for 2D CT with parallel projections or fan-beam the solution is to use an FFT based preconditioner with a cone filter in the image domain, which amplifies high spatial frequencies and helps to accelerate convergence; this has also been shown for unweighted least-square reconstruction in [22].

The idea of designing suitable preconditioners for CT is to exploit the structure of the forward and back operator and, in particular, the filtering in the image domain which can be possible for the 2D parallel beam or fan beam geometry. The

parallel beam CT measurement system is governed by the Radon operator which is a non tight frame so according to the Filtered Back Projection theorem in the image domain [23] the following property of the unitary of the operator holds:

$$\mathbf{A}^T \cdot \mathbf{AV} = \mathbf{I} \tag{16}$$

where $\mathbf{V}$ is the operator that applies the cone filter spatially in the domain of μ.
By applying preconditioning on the CT operator we obtain the coefficient vector and compressed measurement

$$\begin{aligned} \mathbf{x} &= \mathbf{V}^{\frac{1}{2}}\mu \\ \mu &= \mathbf{V}^{-\frac{1}{2}}\mathbf{x} \\ \mathbf{y} &= \mathbf{AV}^{-\frac{1}{2}}\mathbf{x} + \nu \end{aligned} \tag{17}$$

where $\mathbf{x}$ is the corresponding input signal.
Incorporating preconditioning into D-AMP results in the following iterations:

$$\mathbf{x}^{t+1} = D_{\hat{\sigma}^t}((\mathbf{V}^{-\frac{1}{2}}\mathbf{A}^T)r^t + \mathbf{x}^t) \tag{18}$$

$$\begin{aligned} r^t &= \mathbf{v} - (\mathbf{AV}^{-\frac{1}{2}})\mathbf{x}^t + \\ &+ \frac{1}{R} r^{t-1} D'_{\hat{\sigma}^{t-1}}((\mathbf{V}^{-\frac{1}{2}}\mathbf{A}^T)r^{t-1} + \mathbf{x}^{t-1}) \end{aligned} \tag{19}$$

or alternatively

$$\mathbf{x}^{t+1} = D_{\hat{\sigma}^t}(\mathbf{s}^t) \tag{20}$$

$$\begin{aligned} \mathbf{s}^t &= \mathbf{x}^t + \left(\mathbf{V}^{-\frac{1}{2}}\mathbf{A}^T\right)\Big(\mathbf{v} - (\mathbf{AV}^{-\frac{1}{2}})\mathbf{x}^t + \\ &+ \frac{1}{R}\frac{\mathbf{s}^{t-1} - \mathbf{x}^{t-1}}{\mathbf{V}^{-\frac{1}{2}}\mathbf{A}^T} D'_{\hat{\sigma}^t}(\mathbf{s}^{t-1})\Big) \end{aligned} \tag{21}$$

B. Output Poisson noise model: link between PWLS and DCT-GAMP

Many methods have been applied to solve the optimization problem (10), among them gradient-descent methods depend on the Hessian of the data fit term, i.e. $\mathbf{A^TWA}$ which is highly shift-variant due to the large dynamic range of $\mathbf{W}$ which makes it difficult to precondition. Iterative shrinkage (IST) and its accelerated variants (FISTA, M-FISTA) can be applied to solve (10) but the convergence speed is determined by the Lipschitz constant of the data fit term $L = \sigma_{max}(\mathbf{A^TWA})$ where σ_{max} is the maximum eigenvalue. A large value of L leads to small steps and equivalently slow convergence.

One possibility for taking into account the CT noise model is to exploit the Gaussian approximation of the Poisson noise and use a preconditioner based on the following diagonal Majorizing matrix [10] whose derivation comes from solving the PWLS objective function Eq. (10) using a surrogate with a diagonal Hessian matrix upper bounded by

$$\mathbf{D} = \mathrm{diag}\left(\mathbf{A^TWA1}\right) > \mathbf{A^TWA} \tag{22}$$

using the non negativity property of the measurement matrix A. The main problem which comes from this type of preconditioner is that it does not take into account the spatial/Fourier type of properties of the matrix A.

Our aim is to design an approximate message passing based algorithm suitable to solve the optimization problem (10) but more flexible to take into account a wider range of regularizer. Furthermore it is important to stress the fact that the proposed algorithm can be derived even without considering an analytic cost function to optimize but as a fixed point solution of the associated Bethe free energy function of the system or as an Minimum Mean Square Error Estimator (MMSE) in a Bayesian formulation.

IV. Incorporation of Poisson Noise Model in AMP: DCT-AMP

As mentioned in Section III-A the weighting term $\mathbf{W}$ although crucial for improving reconstruction quality poses a challenge due to its large dynamic range. Compared to $\mathbf{A^TWA}$ the term $\mathbf{A^TA}$ tends to be more shift-invariant and better for preconditioning using cone filters. Therefore our idea is to decouple $\mathbf{W}$ from the preconditioning of the CT system based on the CT geometry. In particular this can be done using the cone filter $\mathbf{V}$ in the image domain as the preconditioner and incorporating the CT Poisson noise model as an output channel distribution in the D-AMP formulation [17]. Furthermore AMP assumes the columns of A to have approximately unit l_2 norm and therefore the elements A_{ai}^2 are expected to be very small for large values of m.
DCT-AMP framework can handle essentially:

- incorporate Poisson noise distribution;
- operator A which has l_2 norm not close to 1 (AMP assumes the columns of A to have approximately unit l_2 norm and therefore the elements A_{ai}^2 are expected to be very small for large values of m).

At the core of our proposed DCT-GAMP algorithm are the two functions: $D_\sigma(\cdot)$ which acts as an approximation for the Bayesian MMSE estimation of the image x, and $g_{out}(\cdot)$ which models the noise measurement distribution.
For Minimum Mean Square Error estimation (MMSE) the posterior distribution of $z_a = A_{a*}\mu$ is given by:

$$p(z_a|y_a) = \frac{p(y_a|z_a)p(z_a|p,\tau_p)}{\int p(y_a|z_a)p(z_a|p,\tau_p)dz_a} \tag{23}$$

where z_a represents the a-th component of the output of the linear transform and p is the estimated measurement vector and τ_p its variance. Here τ_x^k can be interpreted as an approximation of the posterior variance of θ_x^k.
If we consider the log-likelihood Poisson noise distribution for the photon counting process

$$p(\mathbf{y}|\mathbf{z}) = \prod_{i=1}^{N} \frac{e^{-[\mathbf{Ax}]_i}[\mathbf{Ax}]_i^{y_i}}{y_i!} \tag{24}$$

or its likelihood, with $z_i = [\mathbf{Ax}]_i$

$$\log p(\mathbf{y}|\mathbf{z}) = \sum_{i=1}^{N} \{-y_i \log(z_i) - z_i\} + \mathrm{const} \tag{25}$$

Algorithm 1: DCT-AMP: Denoising Preconditioned Approximate Message Passing

Initialization: set $k = 0$, $s_a(-1) = 0$

while error $<$ tol **do**

Step 1: for each $a \in [M]$:

$$\begin{aligned} \tau_p^k &= \tfrac{1}{M}\|A\|_F^2 \tau_x^k \\ p_a^k &= A_{a*} V_{*a}^{-\frac{1}{2}} \vartheta_x^k - \tau_p^k r_a^{k-1} \end{aligned}$$

Step 2: for each $a \in [M]$:

$$\begin{aligned} r_a^k &= g_{out}(p_a^k, y_a, \tau_p^k) \\ \sigma^k &= -\tfrac{1}{m}\sum_{a=1}^{m} \tfrac{\partial}{\partial p} g_{out}(s_a^k, y_a, \tau_p^k) \end{aligned}$$

Step 3: for each $i \in [N]$:

$$\begin{aligned} \tfrac{1}{\tau_s^k} &= \tfrac{1}{N}\|A\|_F^2 \sigma^k \\ s_i^k &= \vartheta_{\mu_i}^k + \tau_r^k V_{i*}^{-\frac{1}{2}} A_{*i}^T r^k \end{aligned}$$

Step 4: for each $i \in [N]$:

$$\begin{aligned} \vartheta_{x_i}^{k+1} &= D_\sigma(p_j^k, q_j, \sigma^k) \\ \tau_x^{k+1} &= \tau_\mu^k D'_{\sigma^k}(p_j^k, q_j, \sigma^k) \end{aligned}$$

end

Return μ^k

The output scalar function, $g_{out}(\cdot)$, is related to the conditional expectation of z_a under the posterior distribution: ($g_{out}(\cdot)$ is a scalar function acting on the measurement domain)

$$g_{out}(\mathbf{p}, \mathbf{y}, \tau_p) = \frac{1}{\tau_p}(\mathbf{z}_0 - \mathbf{p}), \quad z_0 = \mathbb{E}[z_a|\mathbf{p}, \mathbf{y}, \tau_p]. \tag{26}$$

where p is the estimate in the measurement domain. In the Appendix A is described the calculation for z_0. An approximation of the Poisson noise is given by using a Gaussian distribution whose mean is data dependent and its variance depends on the expected value, i.e. $\mathcal{N}(\mathbf{Ax}, \mathbf{Ax})$. In our experiment we have found that for the particular dataset the Gaussian approximation is very accurate and this can be justified since for small photon counts photon noise is generally dominated by other signal independent sources of noise and for large counts the central limit theorem ensures that the Poisson distribution approaches a Gaussian. The input function D_σ for MMSE estimation is the conditional expectation of x_i under the posterior distribution:

$$D_\sigma(\mathbf{r}, \mathbf{q}, \sigma) \approx \mathbb{E}[\mathbf{x}|\mathbf{r}, \sigma] = \mathbf{x}^{MMSE} \tag{27}$$

The scaled partial derivative of $\tau_r g_{in}(r, \tau_r)$ is the conditional variance under this distribution:

$$\sigma D'_{in}(\mathbf{r}, \sigma) \approx \mathrm{Var}[\mathbf{x}|\mathbf{r}, \sigma] \tag{28}$$

The MMSE estimation has been replaced by applying a generic non-linear function, a denoiser D_{σ_r} on r. τ_μ^k can be interpreted as an approximation of the posterior variance of μ_i^k. The main reason is that we assume that for large m and N the MSE $\frac{1}{N}\|D_\sigma(p_j^k, q_j, \tau_r^k) - \hat{\mu}\|_2^2$, where $\hat{\mu}$ is the true image, tends to 0 as k increase, at limit to infinity.

V. State Evolution

An important property of D-AMP is the possibility of evaluating its performance through the so called state evolution to keep track of the standard deviation of the MSE $\hat{\sigma}_t$ at each iteration. If we define

$$\begin{aligned} \mathbf{q}^t &= \mathbf{x}^t - \mathbf{x}_0 \\ \mathbf{h}^t &= \mathbf{s}^t - \mathbf{x}_0 \end{aligned}$$

substituting (18) and after some basic algebra we end up with

$$\mathbf{q}^{t+1} = D_{\sigma^t}(\mathbf{x}_0 + \mathbf{h}^t) - \mathbf{x}_0 \tag{29}$$

$$\begin{aligned} \mathbf{h}^t = &(\mathbf{I} - \mathbf{V}^{-\frac{1}{2}}\mathbf{A}^\mathbf{T}\mathbf{W}\mathbf{A}\mathbf{V}^{-\frac{1}{2}})\mathbf{q}^t + \\ &+(\mathbf{V}^{-\frac{1}{2}}\mathbf{A}^T\mathbf{W}^{\frac{1}{2}})\mathbf{n} + \mathbf{h}_{Onsager}^t \end{aligned} \tag{30}$$

$$\begin{aligned} \mathbf{h}_{Onsager}^t = &\frac{N}{M} \cdot \left(\frac{1}{N} \sum_{j=1}^{N} D'_{\sigma^{t-1}}(\mathbf{x}_0 + \mathbf{h}^{t-1}) \right) \cdot \\ &\cdot(\mathbf{h}^{t+1} - \mathbf{q}^{t+1}) \end{aligned} \tag{31}$$

Given (29) the state evolution refers to the following recursion:

$$\vartheta^{t+1} = \mathbb{E}||\mathbf{q}^{t-1}||_2^2 = \mathbb{E}\left\{\left[D_{\sigma^t}(\mathbf{x}_0 + \sigma^t \mathbf{r}^t) - \mathbf{x}_0\right]\right\} \tag{32}$$

$$\sigma^t = \frac{N}{M}\vartheta^t + \sigma_\epsilon \tag{33}$$

which provides an estimate of the MSE at each iteration. Although analysis is only rigorously valid under restricted conditions, we will see in Section VI-B that we have obtained good estimates with real CT experiments.

VI. Experimental Results

In this section, we provide numerical results where we compare the reconstruction quality DCT-AMP. The DCT-AMP framework has been applied for CT reconstruction on real luggage scans obtained using Morpho CTX5500 Air Cargo dual energy system with fan beam CT geometry. This is a single-row scanner with 476 detector channels and a 80cm field of view.

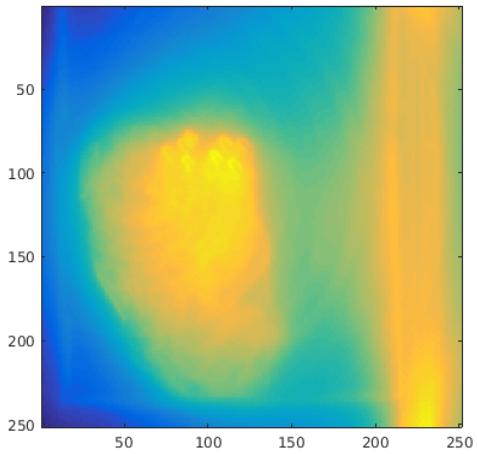

(a) Filtered Back Projection

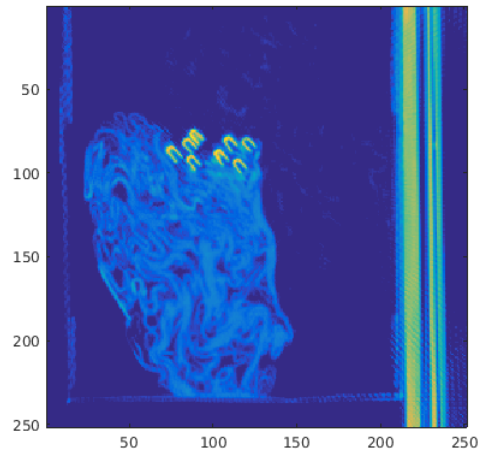

(b) NLM-CT-AMP with cone filter preconditioner and Poisson model

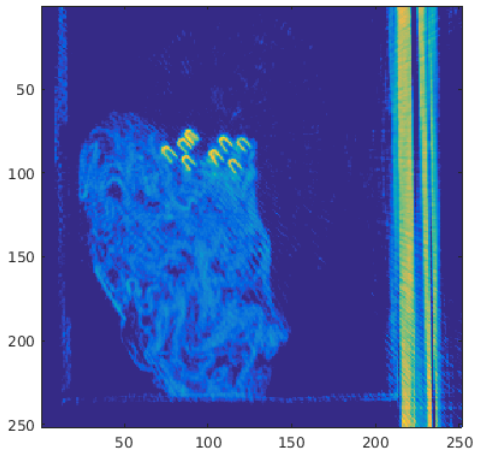

(c) D-GAMP with D noise preconditioner in Eq. (22)

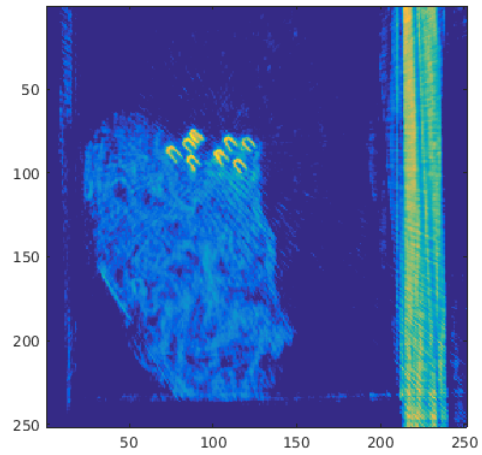

(d) NLM-AMP without Onsager term

Fig. 1: CT image reconstruction of slice 35 using 72 views.

For each slice location, two slices were acquired one at 100 KVp, the other at 198 KVp. Each slice, in full acquisition, has 720 degrees of data, with 720 views/rotation (0.5 degree increments, 1440 views total). The reconstruction has been performed for each energy independently and we will consider only the results obtained for 100 kVp. The reconstructed image is of 512×512 array size. The main objective of simulation is to perform reconstruction with DCT-GAMP on a limited number of views: the results are showing the performance using 72 views regularly undersampled out of the full set of views constituted of 720 views. The preconditioning in the image domain has been obtained designing through a cone filter. The image denoising algorithm Non Local Means (NLM) [24] has been used as the denoiser in DCT-GAMP since it provides good reconstruction performance and keep computation time reasonable compared to the state of the art denoiser BM3D [25]. The number of iterations for DCT-GAMP algorithms has been set to 15 iteration but we will see that the Mean Square Error (taking as reference the FBP with full set of views) decreases rapidly and then tends to stabilize in under 10 iterations. As reference in the Figure 1a we show the reconstruction, using 72 views, and Filtered Back Projection.

A. *Role of the preconditioner and the Onsager term*

In order to evaluate the different preconditioners and empirically demonstrate the intuition that decoupling the system and noise preconditioner leads to reconstruction improvement, we have performed the reconstruction of slice 35 from the Cargo 3D dataset using a cone filter preconditioner and the Poisson noise model and the result is shown in Fig. 1b.

Fig. 1c depicts the reconstruction using the majorization matrix for $\mathbf{AWA}^T$ and both qualitatively and quantitatively we can notice a degradation of the reconstruction.

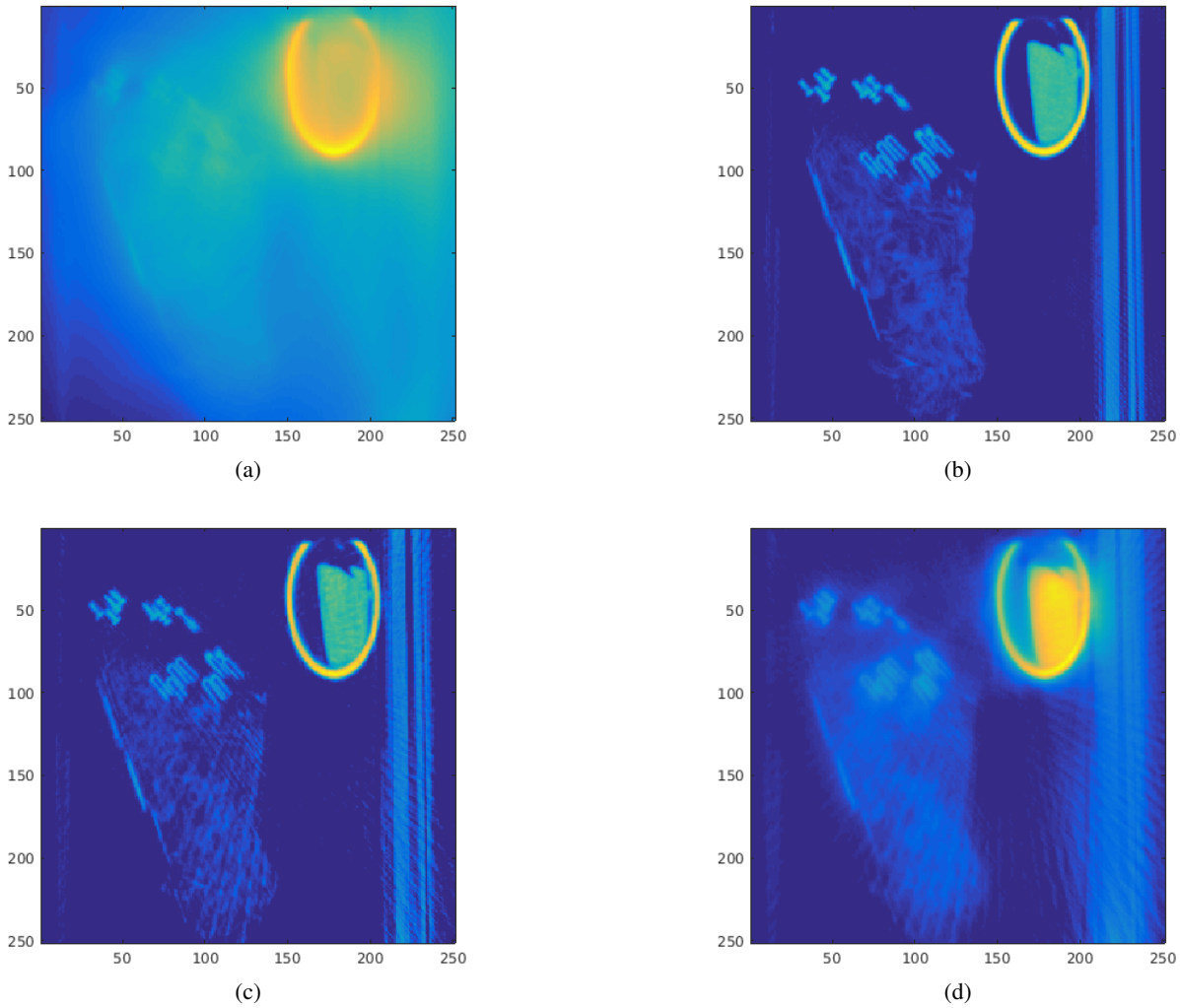

Fig. 2: CT image reconstruction of slice 22 using a) FBP, b) NLM-AMP; c) D preconditioner; d) NLM-AMP without Onsager term.

Finally we have evaluated the role of the Onsager term in the DCT-AMP algorithm to check whether it improves the reconstruction. Without the Onsager term the AMP algorithm behaves like a denoising iterative thresholding algorithm. The reconstruction without the Onsager term is shown in Fig. 1d.

For a quantitative comparison we have chosen the PSNR as the metric. In order to quantify the reconstruction quality of each algorithm, the peak signal to noise ratio (PSNR) of each 2D reconstructed slice is measured. The PSNR is defined as the ratio between the maximum squared value of the FBP with the full number of projections and the mean square error of the estimation. In table I are reported the results.

Another important observation is how it is important the role of the Onsager term even in the case of CT reconstruction. To show the consistency of the results, in Figure 2 the same comparison has been run on a different z section (slice 22) of the CT scan. Analysing the results in Table I it is possible to infer that the use of the Cone filter always outperforms the D preconditioner both in terms of PSNR on the region of interest, depicted in the figures, and running time. Furthermore the use of NLM denoiser yields to better PSNR compared to TV denoiser but with a cost of higher computational time. Finally

TABLE I: PSNR for different preconditioners

Algorithms	**PSNR** [dB]	**Time**
NLM-CT-AMP Cone Filter	68.15	6.1 min
NLM-CT-AMP with D preconditioner	62.06	7.5 min
NLM-CT-AMP with Cone Filter and without Onsager term	59.5	4.1 min
TV-CT-AMP Cone Filter	61.5	4.3 min
TV-FISTA with Cone filter and OS	59.7	5.1 min
TV-FISTA with D preconditioner and OS	56.9	5.6 min

it is important to stress that the TV based AMP with Cone filter preconditioner achieves better performances in term of time and reconstruction quality compared to other optimization algorithm like TV-FISTA.

Although the DCT-AMP formulation allows to exploit more complex priors, it is important to show how AMP, as an iterative optimization algorithm, performs for solving the PWLS cost function 10 using a Total Variation regularization term and compare in terms of computational time and PSNR with FISTA using the deterministic subgradient technique, called Ordered subset to reduce the running time. In the following numerical experiment we show the results running TV-CT-AMP on 2D fan beam, using the package [26], and FISTA [8] and computing the gradient on a lower dimensional space, i.e. for each outer iteration of the algorithm a block subset of measurements y of dimension 16 is processed. One outer iteration is composed of applying the gradient descent iteration on contiguously blocks until each element of the high dimensional space is processed at least once. In Figure 3 we show the reconstructed results and in Table I the computational time: for FISTA we have used 80 iterations since it was the minimum number to reach convergence for this particular dataset.

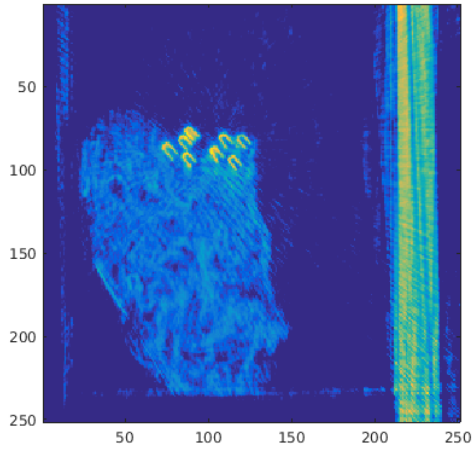

Fig. 3: comparison TV-CT-AMP reconstruction and FISTA for solving PWLS problem. (colour)

B. State Evolution Analysis

An important feature of DCT-AMP is the possibility of checking how good the estimate is, at each iteration. Not only does this provide an estimate of uncertainty within the algorithm, it also allows the algorithm to exploit this knowledge through the Onsager term. If accurate, this term improves the performance and convergence rate of the algorithm. In particular given the actual MSE estimate, taking as reference the full views FBP reconstruction, we can calculate the predicted MSE at the next iteration and compare with the actual estimate.
Our empirical results run on experimental data acquired using the 2D fan beam CT geometry show that the state evolution based on the previous estimate can predict with good precision

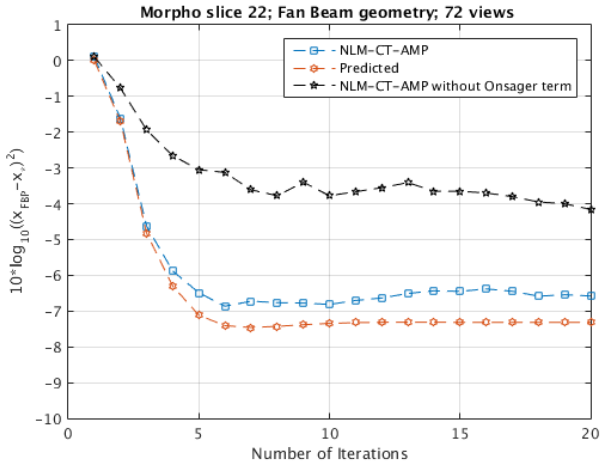

Fig. 4: Deterministic state evolution and MSE estimates using NLM-CT-AMP with and without Onsager term

the Mean Square Error (MSE) of NLM-CT-AMP as depicted in Figure 4. In particular considering the first iterations the actual MSE of NLM-CT-AMP is very close with the predicted one, after 10 iteration the current estimate tends to be higher, between 0.7-1.2 dB compared with the state evolution prediction but overall we can claim that we can achieve a good prediction. Note that the the Onsager term is omitted, the state evolution is no longer a good MSE predictor and the performance is significantly deteriorated.

VII. Conclusions

In this work we have presented a proof of concept for using Approximate Message passing type of iterative algorithms for solving inverse problems with a structured measurement matrix and in particular for X-ray CT reconstruction. The proposed framework replies of the design of an appropriate preconditioner for the ill-conditioned measurement matrix and a statistical model for the measurement noise. In addition, exploiting the flexibility of the generalized AMP we can decouple the action of the preconditioner from the noise. We have experimentally shown the important role of the Onsager term regarding reconstruction performance improvement and the ability of the state evolution analysis to estimate the current MSE through the iterations. Numerical results on experimental Cargo data demonstrate how the DCT-AMP framework can be a promising iterative algorithm for CT reconstruction, yielding to faster reconstruction compared to methods such as FISTA for solving the PWLS problem. In addition DCT-AMP allows different prior image models to be used on the signal by employing different denoisers. Further acceleration of the DCT-AMP algorithm could be made by employing the idea of approximating the gradient descent step on a low-dimensional space, utilizing the Ordered Subset principle, but its implementation is not straightforward due to the Onsager term and is left for future research.

ACKNOWLEDGMENT

This work was supported by U.S. Department of Homeland Security, Science and Technology Directorate, Explosives Division, BAA 13-05, Contract # HSHQDC-14-C-B0048. Alessandro Perelli acknowledges partial support from EPSRC platform grant EP/J015180/1. The authors thank Walter Garms, Morpho Detection Inc., for providing real CT datasets.

APPENDIX

We consider a Poisson likelihood distribution for the noise model with non-informative prior as following

$$p(\mathbf{p}|\mathbf{z}) = \prod_{i=1}^{N} \frac{e^{-z_i} {z_i}^{y_i}}{p_i!} \tag{34}$$

and supposing p_i independent from z_i we obtain

$$p(\mathbf{p}|\mathbf{z}) = \frac{e^{-N\cdot\mathbb{E}[\mathbf{z}]}\cdot z^{N\cdot\mathbb{E}[\mathbf{p}]}}{\prod_{i=1}^{N} p_i!} \tag{35}$$

The fisher information is

$$\begin{aligned}
\mathcal{I}(\mathbf{z}) &= -\mathbb{E}\left[\frac{\partial^2}{\partial \mathbf{z}^2}\log p(\mathbf{p}|\mathbf{z})\middle|\mathbf{z}\right] = \\
&= -\mathbb{E}\left[\frac{\partial^2}{\partial \mathbf{z}^2}\left(N\cdot\mathbb{E}[\mathbf{p}]\log\mathbf{z} - n\mathbf{z}\right)\middle|\mathbf{z}\right] + \\
&= -\mathbb{E}\left[-\frac{N\mathbb{E}[\mathbf{p}]}{\mathbf{z}^2}\middle|\mathbf{z}\right] = \frac{N}{\mathbf{z}}
\end{aligned}$$

So the Jeffreys prior is

$$p(\mathbf{z}) \propto \frac{1}{\sqrt{\mathbf{z}}} \tag{36}$$

which follows a Gamma distribution $\mathrm{Gamma}(\alpha,\beta)$ with parameter $\alpha = \frac{1}{2}$ and $\beta = 0$. Moreover the posterior can be obtained using the conjugacy of the Gamma distribution relative to the Poisson likelihood:

$$\begin{aligned}
p(\mathbf{z}|\mathbf{p}) &\propto p(\mathbf{p}|\mathbf{z})p(\mathbf{z}) = \mathbf{z}^{N\cdot\mathbb{E}[\mathbf{p}]}\cdot e^{-N\mathbf{z}}\cdot z^{-\frac{1}{2}} \\
&= \mathbf{z}^{N\cdot\mathbb{E}[\mathbf{p}]-\frac{1}{2}}\cdot e^{-N\mathbf{z}} = \mathrm{Gamma}\Big(\frac{1}{2}+N\mathbb{E}[\mathbf{p}], N\Big)
\end{aligned}$$

and finally

$$\mathbf{z}_0 = \mathbb{E}[\mathbf{z}|\mathbf{p}] = \mathbb{E}[\mathbf{p}] + \frac{1}{2N} \tag{37}$$

REFERENCES

[1] B. Gonzales, D. Spronk, Y. Cheng, A. Tucker, M. Beckman, O. Zhou, and J. Lu, "Rectangular fixed-gantry CT prototype: combining cnt X-ray sources and accelerated compressed sensing-based reconstruction," *IEEE Access*, vol. 2, pp. 971–981, 2014.

[2] I. A. Elbakri and J. A. Fessler, "Statistical image reconstruction for polyenergetic X-ray computed tomography," *IEEE Transactions on Medical Imaging*, vol. 21, no. 2, pp. 89–99, 2002.

[3] J.-B. Thibault, K. Sauer, C. Bouman, and J. Hsieh, "A three-dimensional statistical approach to improved image quality for multislice helical CT," *Medical physics*, vol. 34, no. 11, pp. 4526–4544, 2007.

[4] K. Sauer and C. Bouman, "A local update strategy for iterative reconstruction from projections," *IEEE Transactions on Signal Processing*, vol. 41, no. 2, pp. 534–548, 1993.

[5] Z. Yu, J.-B. Thibault, C. Bouman, K. Sauer, and J. Hsieh, "Fast model-based X-ray CT reconstruction using spatially nonhomogeneous ICD optimization," *IEEE Transactions on Image Processing*, vol. 20, no. 1, pp. 161–175, 2011.

[6] J. A. Fessler and S. Booth, "Conjugate-gradient preconditioning methods for shift-variant pet image reconstruction," *IEEE Transactions on Image Processing*, vol. 8, no. 5, pp. 688–699, 1999.

[7] H. Erdogan and J. A. Fessler, "Ordered subsets algorithms for transmission tomography," *Physics in medicine and biology*, vol. 44, no. 11, pp. 2835, 1999.

[8] S. Ramani and J. A. Fessler, "A splitting-based iterative algorithm for accelerated statistical X-ray ct reconstruction," *IEEE Transactions on Medical Imaging*, vol. 31, no. 3, pp. 677–688, 2012.

[9] S. Y. Chun, Y. Dewaraja, and J. A. Fessler, "Alternating direction method of multiplier for tomography with nonlocal regularizers," *IEEE Transactions on Medical Imaging*, vol. 33, no. 10, pp. 1960–1968, 2014.

[10] D. Kim, S. Ramani, and J. A. Fessler, "Combining ordered subsets and momentum for accelerated X-ray ct image reconstruction," *IEEE Transactions on Medical Imaging*, vol. 34, no. 1, pp. 167–178, 2015.

[11] D. L. Donoho, A. Maleki, and A. Montanari, "Message-passing algorithms for compressed sensing," *Proceedings of the National Academy of Sciences*, vol. 106, no. 45, pp. 18914–18919, 2009.

[12] S. Rangan, P. Schniter, and A. Fletcher, "On the convergence of approximate message passing with arbitrary matrices," in *IEEE International Symposium on Information Theory (ISIT)*. IEEE, 2014, pp. 236–240.

[13] S. Rangan, A. K. Fletcher, P. Schniter, and U. Kamilov, "Inference for generalized linear models via alternating directions and Bethe free energy minimization," in *2015 IEEE International Symposium on Information Theory (ISIT)*. IEEE, 2015, pp. 1640–1644.

[14] J. Tan, Y. Ma, H. Rueda, D. Baron, and G. R. Arce, "Compressive hyperspectral imaging via approximate message passing," *IEEE Journal of Selected Topics in Signal Processing*, vol. 10, no. 2, pp. 389–401, March 2016.

[15] B. Cakmak, O. Winther, and B. H. Fleury, "S-AMP: Approximate message passing for general matrix ensembles," in *IEEE Information Theory Workshop (ITW)*, 2014, pp. 192–196.

[16] M. Nilchian, C. Vonesch, P. Modregger, M. Stampanoni, and M. Unser, "Fast iterative reconstruction of differential phase contrast X-ray tomograms," *Optics express*, vol. 21, no. 5, pp. 5511–5528, 2013.

[17] S. Rangan, "Generalized approximate message passing for estimation with random linear mixing," in *IEEE International Symposium on Information Theory Proceedings*, 2011, pp. 2168–2172.

[18] C. A. Metzler, A. Maleki, and R. G. Baraniuk, "From denoising to compressed sensing," *arXiv preprint arXiv:1406.4175*, 2014.

[19] C. H. Yan, R. Whalen, G. Beaupre, S. Yen, and S. Napel, "Reconstruction algorithm for polychromatic CT imaging: application to beam hardening correction," *IEEE Transactions on Medical Imaging*, vol. 19, no. 1, pp. 1–11, 2000.

[20] B. Whiting, P. Massoumzadeh, O. Earl, J. O'Sullivan, D. Snyder, and J. Williamson, "Properties of preprocessed sinogram data in X-ray computed tomography," *Medical physics*, vol. 33, no. 9, pp. 3290–3303, 2006.

[21] S. Ramani, T. Blu, and M. Unser, "Monte-carlo SURE: A black-box optimization of regularization parameters for general denoising algorithms," *IEEE Transactions on Image Processing*, vol. 17, no. 9, pp. 1540–1554, 2008.

[22] N. H. Clinthorne, T. S. Pan, P. C. Chiao, W. L. Rogers, and J. A. Stamos, "Preconditioning methods for improved convergence rates in iterative reconstructions," *IEEE Transactions on Medical Imaging*, vol. 12, no. 1, pp. 78–83, Mar 1993.

[23] S. Matej, J. A. Fessler, and I. G. Kazantsev, "Iterative tomographic image reconstruction using Fourier-based forward and back-projectors,"

IEEE Transactions on Medical Imaging, vol. 23, no. 4, pp. 401–412, 2004.

[24] A. Buades, B. Coll, and J-M. Morel, "A non-local algorithm for image denoising," in *2005 IEEE Computer Society Conference on Computer Vision and Pattern Recognition (CVPR'05)*. IEEE, 2005, vol. 2, pp. 60–65.

[25] K. Dabov, A. Foi, V. Katkovnik, and K. Egiazarian, "Image denoising by sparse 3-d transform-domain collaborative filtering," *IEEE Transactions on Image Processing*, vol. 16, no. 8, pp. 2080–2095, 2007.

[26] M. Figueiredo, J. Dias, J. Oliveira, and R. Nowak, "On total variation denoising: A new majorization-minimization algorithm and an experimental comparisonwith wavalet denoising," in *2006 International Conference on Image Processing*. IEEE, 2006, pp. 2633–2636.